

1 **Supplementary Information**

2 Response of the North Atlantic surface and intermediate ocean structure to climate warming
3 of MIS 11

4
5 Evgenia S. Kandiano^{1,2*}, Marcel T. J. van der Meer¹, Stefan Schouten^{1,3} Kirsten Fahl⁴, Jaap
6 S. Sinninghe Damsté^{1,3}, and Henning A. Bauch^{2,4}

7
8 ¹Department of Marine Microbiology and Biogeochemistry, NIOZ Netherlands Institute for
9 Sea Research, and Utrecht University, Den Burg, NL-1790 AB, the Netherlands

10 ²Department of Paleoceanography, GEOMAR Helmholtz Centre for Ocean Research Kiel,
11 Kiel, D-24148, Germany

12 ³Faculty of Geosciences, Utrecht University, Utrecht, NL-3584 CD, the Netherlands

13 ⁴Department of Marine Geology, Alfred Wegener Institute Helmholtz Centre for Polar and
14 Marine Research, Bremerhaven, D-27568, Germany

15
16 *To whom correspondence should be addressed. Email: ekandiano@geomar.de

17 18 **Core sampling**

19 The core section covering the full interglacial period of MIS 11ss was sampled continuously
20 as 0.5 cm slabs while the section covering Termination V was sampled as 1 cm slabs. All
21 samples were freeze dried. For organic and inorganic analyses different sets of samples
22 were used. All inorganic analyses were produced with 1-cm resolution while GDGT-based
23 TEX₈₆ SST reconstructions were performed in 2 cm resolution and increased to 1 cm
24 resolution where necessary. Alkenone distributions and hydrogen isotope compositions were
25 measured on the same sample set as GDGT, but only in those samples where sufficient
26 amounts of alkenones were found. For comparison, all organic analyses have also been
27 performed on the core top sample (Fig. S1A, B; See also section Methods).

28
29
30
31
32
33
34
35
36
37
38
39
40
41
42
43
44
45
46
47
48
49
50
51
52
53
54

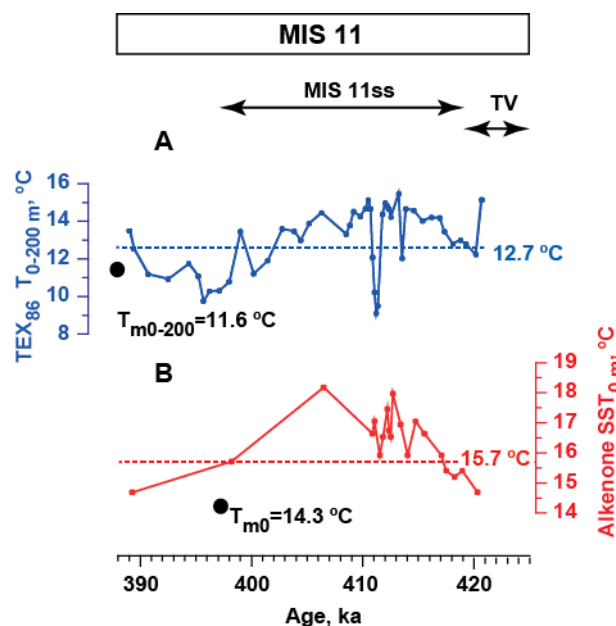


Figure S1. Temperature reconstructions during MIS 11 in comparison with modern values and temperature reconstructions in the core top sample. A: TEX₈₆^L temperature reconstructions for 0-200 m water depth along with modern summer temperature of the same depth indicated by black dot (11.6 °C²⁶), dashed line indicates the result of the TEX₈₆^L (0-200 m) temperature reconstruction from the core top sample (12.7 °C). B: U₃₇^{K'} SST reconstructions for 0 m water depth along with modern summer temperature of the same depth indicated by black dot (14.3 °C²⁶). Dashed line indicates the result of the U₃₇^{K'} reconstruction from the core top sample (15.7 °C). MIS 11, MIS 11ss and Termination V (TV) are indicated on the top panel.

Sample preparation for inorganic analyses

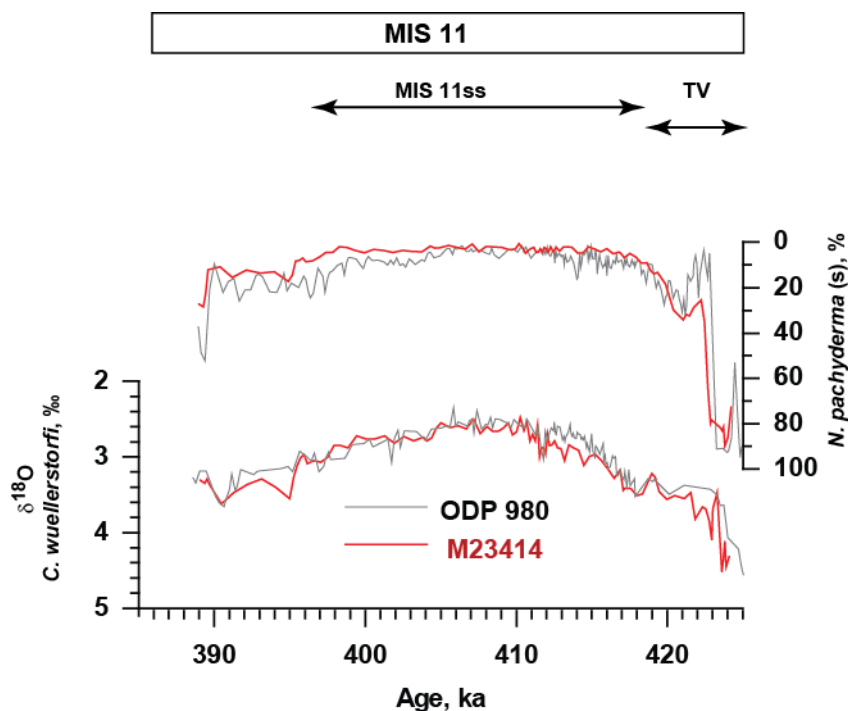
Freeze dried samples were washed over 63 µm mesh-sized sieve in deionized water, dried in an oven under 40 °C. Fraction >150 µm was used.

Sample preparation for organic analyses

Total lipid extracts from freeze-dried samples were generated using Accelerated Solvent Extractor (DIONEX AS E350, 100 °C) with a mixture of dichloromethane (DCM): methanol (MeOH, 9:1 v/v). The extracts were separated into apolar, alkenone and polar fractions using Al₂O₃ columns with hexane: DCM (9:1 v/v), hexane:DCM (1:1 v/v), and DCM:MeOH (1:1 v/v), respectively.

Age model

55 The age model of core M23414 was established using using benthic $\delta^{18}\text{O}$ ⁴ (Fig. S2; The age
 56 model of a nearby ODP core 980⁵ was tuned to the M2414 age model). MIS 11ss is
 57 identifiable between ~ 419 and 397 ka by a drastic decrease of the IRD content, high
 58 temperature values as well as low benthic and planktic oxygen isotope values, (Fig. 2). IRD,
 59 however, remained present during the interglacial, although in much smaller, variable
 60 amounts (Fig. 2).



73 Figure S2. Relative abundance of *N. pachyderma* (s) and benthic $\delta^{18}\text{O}$ from core
 74 M23414⁵ (red lines) and ODP Site 980⁴ (grey lines). The age model of ODP 980 was
 75 tuned to the age model of M23414.

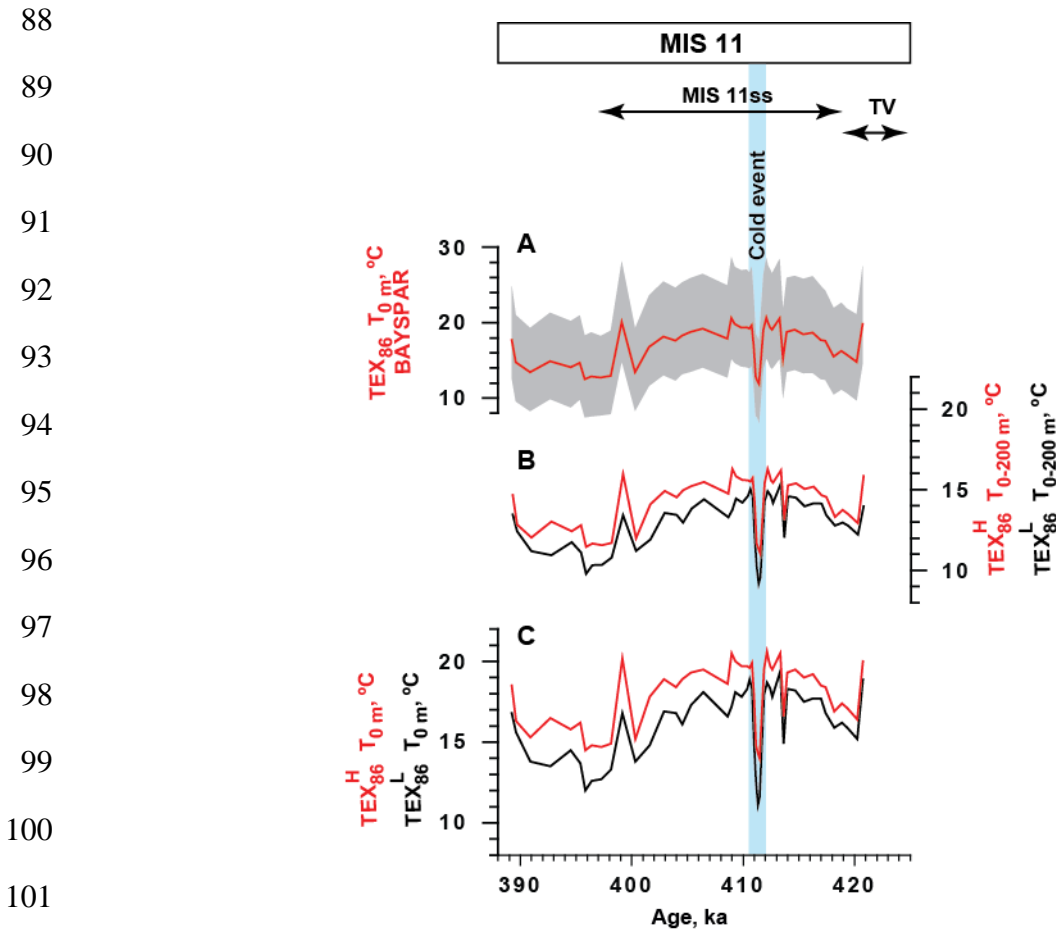
76 Comparison of TEX_{86} derived temperature estimates

77 In order to show that the cold event found by us is not an artifact of the calibration, we have
 78 calculated temperatures according to a variety of different widely used calibrations:

79 – TEX_{86}^L equation⁶ calibrated towards temperature in subsurface water (0-200m;

80 $T=50.8 \cdot \log \text{TEX}_{86}^L + 36.1$, where T is temperature). This record is used in the main text;

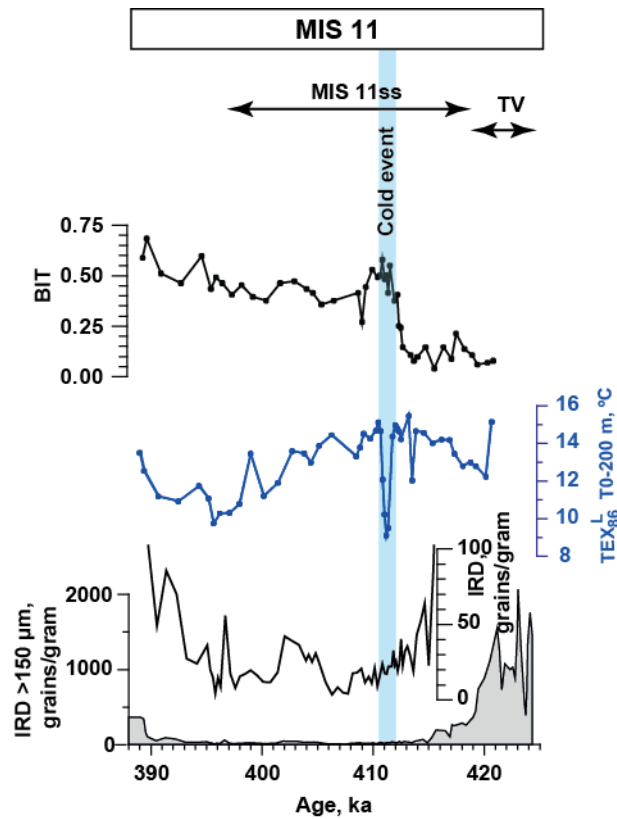
81 – $\text{TEX}_{86}^{\text{H}}$ equation⁷ calibrated towards temperature in subsurface water (0-200m;
 82 $T=54.7*\log\text{TEX}_{86}^{\text{H}} +30.7$, where T is temperature);
 83 – $\text{TEX}_{86}^{\text{H}}$ equation⁸ calibrated to SST (0 m; $\text{SST}=68.4*\log\text{TEX}_{86}^{\text{H}} +38.69$);
 84 – $\text{TEX}_{86}^{\text{L}}$ equation⁸ calibrated to SST (0 m; ($\text{SST}=67.5*\log\text{TEX}_{86}^{\text{L}}+46.9$);
 85 – Bayspar calibration⁹ for TEX_{86} calibrated to SST (0 m).
 86 Application of all calibrations yielded the same temperature trends but differed in absolute
 87 values (Fig. S3).



102 Figure S3. Comparison of TEX_{86} temperature reconstructions derived from different
 103 calibrations. Blue bar indicates cold event. MIS 11 and Termination V (TV) are indicated
 104 on the top panel. A: Bayspar surface temperature reconstructions according to ref. 9.
 105 Mean values are shown by the line while shaded area includes 90 % confidence interval;
 106 B: $\text{TEX}_{86}^{\text{L}}$ (black line) and $\text{TEX}_{86}^{\text{H}}$ (red line) temperature reconstructions for 0-200 m
 107 water depth layer according to ref. 6, 8; C:
 $\text{TEX}_{86}^{\text{L}}$ (black line) and $\text{TEX}_{86}^{\text{H}}$ (red line) temperature reconstructions for 0 m water
 depth according to ref. 8.

108 **BIT index**

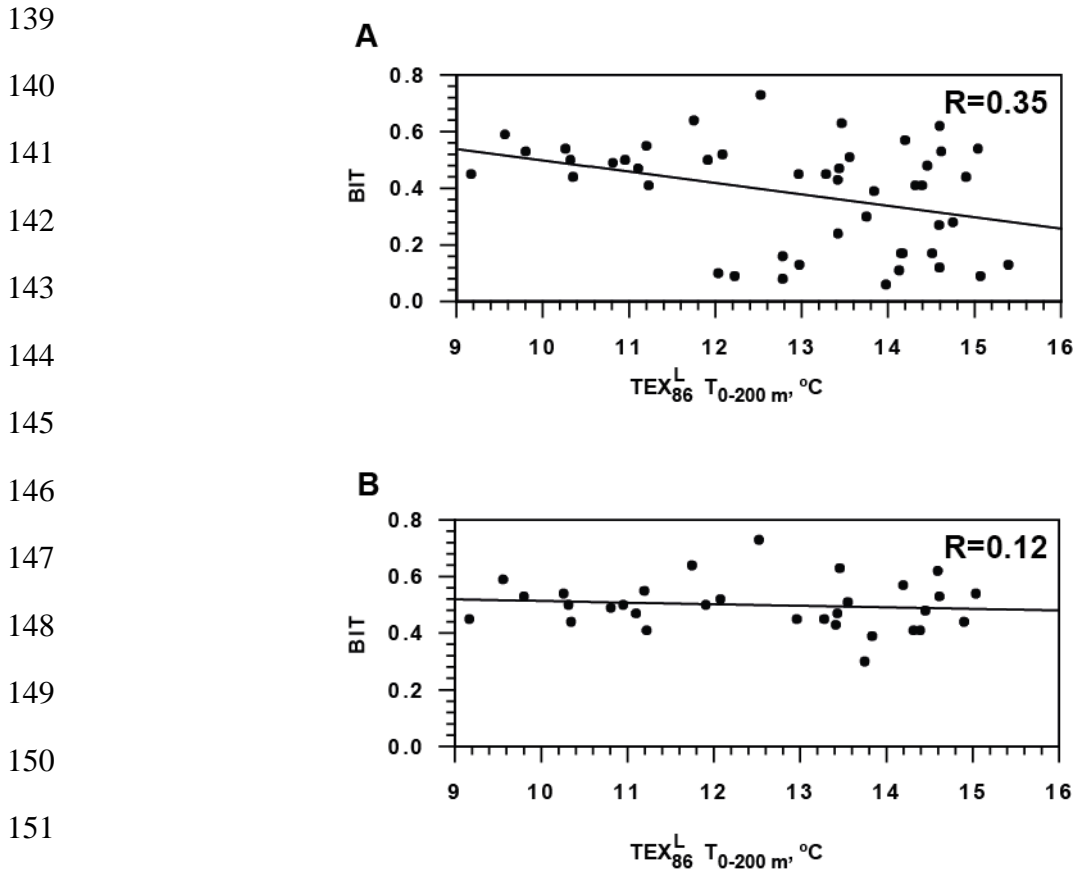
109 The TEX_{86} proxy is known to be affected by terrestrial input which in this region will be mainly
110 transported by ice rafted debris¹⁰. To constrain the effect of terrestrial input, the Branched
111 and Isoprenoid Tetraether (BIT) indices were calculated according to ref. 11 (Fig. S4).



126 Figure S4. BIT indices in core M23414 along with TEX_{86}^L temperature reconstructions for
127 0-200 m water depth layer and IRD⁵ (note different scales for IRD on the left and right
128 panels) across MIS 11. Blue bar indicates cold event. MIS 11 and Termination V (TV)
129 are indicated on the top panel.

130 The BIT index shows relatively high values for most of MIS 11, possibly due to IRD input¹⁰.
131 Alternatively, the organic matter in the sediments were exposed to oxygen and thus oxidized.
132 Oxidic degradation is known to increase the BIT index due to the better preservation of
133 terrestrial GDGTs¹². However, the impact of allochthonous organic matter input on the
134 obtained temperature reconstruction is likely relatively small as we found only a low
135 correlation between BIT and TEX_{86}^L 0-200m temperature estimates for the total MIS 11 period

136 (Fig. S5A) as well as for its later part, where the BIT exceed the cut off value of 0.3¹³ (Fig.
 137 S5B). The absence of a strong correlation suggests no major impact of terrestrial GDGTs on
 138 the TEX₈₆, at least not for the observed cold event.



153 Figure S5. Correlation between TEX₈₆^L temperature reconstructions for 0-200 m water
 154 depth layer and BIT indices in core M23414 across MIS 11. A: the correlation includes
 155 all TEX₈₆^L_{0-200m} data; B: the correlation comprises only those TEX₈₆^L_{0-200m} temperature
 156 estimates in which BIT indices exceed the critical value of 0.3¹³.

156 Comparison of the two alkenone $U_{37}^{K'}$ SST records

157 Comparison between our new results and those of a previously published $U_{37}^{K'}$ SST record of
 158 the same core³ (Fig. 2, black line) displays a temperature difference of on average 2°C. This
 159 difference is likely due to the slight differences between the extraction method and
 160 instrumental conditions used in the different laboratories, in combination with very low
 161 alkenone concentrations (< 300ng/g sed). These interlaboratory differences have already

162 been discussed¹⁴. However, since we mainly focus on the trends in the temperature record,
163 this offset is not affecting our interpretations.

164

165 **Salinity reconstructions derived from δD analysis of alkenones**

166 Culture experiments have shown that the δD value of alkenones is mainly dependent on
167 salinity and the hydrogen isotopic composition of growth water which is also related to
168 salinity and in a minor degree on a growth rate of alkenone producers^{15,16}. A change of 4-5 ‰
169 in alkenone δD corresponds to a change of one salinity unit and combines both the biological
170 response to salinity and a 1.7 ‰ δD change of the water^{15,17}. In natural environments the
171 relation between salinity and δD of water is not constant in space and time and can change
172 with global ice volume changes due to its effect on a δD water composition¹⁸, but also with
173 changes in evaporation and precipitation balances. The observed intra-interglacial MIS 11ss
174 cold event occurred at the very end of the global ice volume decrease and, therefore, the
175 effect of ice volume changes on alkenone δD composition is most likely negligible. According
176 to the modern distribution of δD values in the North Atlantic, the waters of the NAC have up
177 to 6 ‰ higher δD values in comparison to the adjacent SPG waters¹⁹. If, by analogy to the
178 modern state, we assume that the maximum δD depletion in surface waters at the site of
179 M23414 associated with the MIS 11ss cold event might reach 6 ‰ due to the expansion of
180 the western waters to the east, this would agree well with the 15 ‰ drop of alkenone δD
181 observed during the cold event as based on the relation described in ref. 15.

182

183 Another cause of a sharp change in the alkenone δD values preceding the cold event could
184 be a change in a species composition of alkenone producers. The Mid-Pleistocene species
185 composition of coccolithophores at Site 980, in the close vicinity to site M23414, revealed
186 only one dominant species *Gephyrocapsa oceanica* which produces alkenones²⁰. However, it
187 was also shown that during cold episodes the cold water indicative species *Coccolithus*
188 *pelagicus* can occur in this region in relatively large amounts. Therefore this species
189 potentially could compete with *G. oceanica* during the MIS 11ss cold event^{21,21}. Although it is

190 thought that *C. pelagicus* does not produce alkenones, a correlation between the abundance
191 of this species and alkenone amounts has been reported²². Therefore, a contribution of
192 another species to changes in alkenone δD cannot completely be ruled out.

193

194 **Ecological preferences of planktic foraminiferal species *G. bulloides* and *T.*** 195 ***quinqueloba***

196 For this study two species with certain ecological preferences were selected: *G. bulloides*
197 and *T. quinqueloba*. Geographical distributions of both species are given in Fig. S6.

198 According to core top samples foraminiferal data base, both species have elevated
199 abundances in relatively cold and fresh productive waters of the SPG situated westward from
200 site M23414²³. Their elevated abundances were also found at frontal zones in the Nordic
201 seas both in surface sediments²⁴ and water column²⁵.

202

203

204

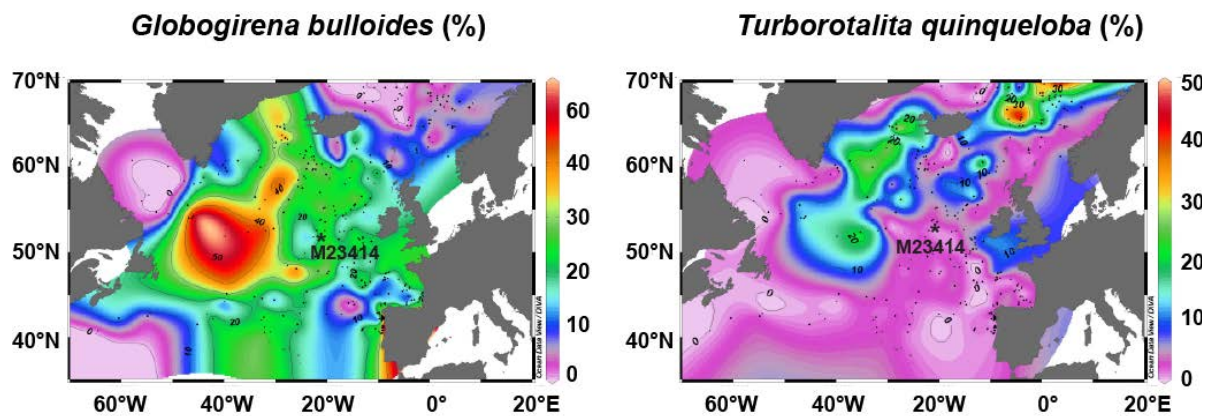
205

206

207

208

209



210 Figure S6. Geographical distribution of planktic foraminiferal species *T. quinqueloba* and *G.*
211 *bulloides*. Map was created using the free program Ocean Data View, Version ODV 4.7.2
(available at web site odv.awi.de) and distribution of planktic foraminifera in core top
212 samples according to ref. 23.

212

213 **References**

- 214 1 Helmke, J. P. & Bauch, H. A. Glacial-interglacial relationship between carbonate
215 components and sediment reflectance in the North Atlantic. *Geo-Marine Letters* **21**, 16-
216 22 (2001).

- 217 2 Helmke, J. P., Schulz, M. & Bauch, H. A. Sediment color record reveals patterns of
218 millennial-scale climate variability over the last 500,000 years. *Quat. Res.* **57**, 16-22
219 (2002).
- 220 3 Kandiano, E. S. *et al.* The meridional temperature gradient in the eastern North Atlantic
221 during MIS 11 and its link to the ocean-atmosphere system. *Palaeogeography*
222 *Palaeoclimatology Palaeoecology* **333**, 24-39 (2012).
- 223 4 Kandiano, E. S. & Bauch, H. A. Phase relationship and surface water mass change in
224 the northeast Atlantic during marine isotope stage 11 (MIS 11). *Quat. Res.* **68**, 445-45
225 (2007).
- 226 5 Oppo, D. W., McManus, J. F. & Cullen, J. L. Abrupt climatic events 500,000 to 340,000
227 years ago: Evidence from subpolar North Atlantic sediments. *Science* **279**, 1335-1338
228 (1998).
- 229 6 Kim, J.-H. *et al.* Holocene subsurface temperature variability in the eastern Antarctic
230 continental margin. *Geophysical Research Letters* **39**, 10.1029/2012gl051157 (2012).
- 231 7 Kim, J.-H. *et al.* Pronounced subsurface cooling of North Atlantic waters off Northwest
232 Africa during Dansgaard–Oeschger interstadials. *Earth and Planetary Science Letters*
233 **339**, 95-102 (2012).
- 234 8 Kim, J.-H. *et al.* New indices and calibrations derived from the distribution of
235 crenarchaeal isoprenoid tetraether lipids: Implications for past sea surface temperature
236 reconstructions. *Geochimica et Cosmochimica Acta* **74**, 4639-4654 (2010).
- 237 9 Tierney, J. E. & Tingley, M. P. A Bayesian, spatially-varying calibration model for the
238 TEX86 proxy. *Geochimica et Cosmochimica Acta* **127**, 83-106 (2014).
- 239 10 Schouten, S., Ossebaer, J., Brummer, G. J., Elderfield, H. & Damsté, J. S. S. Transport
240 of terrestrial organic matter to the deep North Atlantic Ocean by ice rafting. *Organic*
241 *Geochemistry* **38**, 1161-1168 (2007).
- 242 11 Hopmans, E. C. *et al.* A novel proxy for terrestrial organic matter in sediments based
243 on branched and isoprenoid tetraether lipids. *Earth and Planetary Science Letters* **224**,
244 107-116 (2004).

- 245 12 Huguet, C. *et al.* Selective preservation of soil organic matter in oxidized marine
246 sediments (Madeira Abyssal Plain). *Geochimica Et Cosmochimica Acta* **72**, 6061-6068
247 (2008).
- 248 13 Weijers, J. W. H., Schouten, S., Spaargaren, O. C. & Damsté, J. S. S. Occurrence and
249 distribution of tetraether membrane lipids in soils: Implications for the use of the TEX86
250 proxy and the BIT index. *Organic Geochemistry* **37**, 1680-1693 (2006).
- 251 14 Rosell-Melé, A. *et al.* Precision of the current methods to measure the alkenone proxy
252 U-37(K') and absolute alkenone abundance in sediments: Results of an interlaboratory
253 comparison study. *Geochemistry Geophysics Geosystems* **2**, 1046 (2001).
- 254 15 Schouten, S. *et al.* The effect of temperature, salinity and growth rate on the stable
255 hydrogen isotopic composition of long chain alkenones produced by *Emiliana huxleyi*
256 and *Gephyrocapsa oceanica*. *Biogeosciences* **3**, 113-119 (2006).
- 257 16 M'Boule, D. *et al.* Salinity dependent hydrogen isotope fractionation in alkenones
258 produced by coastal and open ocean haptophyte algae. *Geochimica Et Cosmochimica*
259 *Acta* **130**, 126-135 (2014).
- 260 17 van der Meer, M. T. J., Benthien, A., Bijma, J., Schouten, S. & Damsté, J. S. S.
261 Alkenone distribution impacts the hydrogen isotopic composition of the C-37:2 and C-
262 37:3 alkan-2-ones in *Emiliana huxleyi*. *Geochimica Et Cosmochimica Acta* **111**, 162-
263 166 (2013).
- 264 18 Rohling, E. J. Paleosalinity: confidence limits and future applications. *Marine Geology*
265 **163**, 1-11 (2000).
- 266 19 Englebrecht, A. C. & Sachs, J. P. Determination of sediment provenance at drift sites
267 using hydrogen isotopes and unsaturation ratios in alkenones. *Geochimica Et*
268 *Cosmochimica Acta* **69** (2005).
- 269 20 Marino, M., Maiorano, P. & Flower, B. P. Calcareous nannofossil changes during the
270 Mid-Pleistocene Revolution: Paleoecologic and paleoceanographic evidence from
271 North Atlantic Site 980/981. *Palaeogeography Palaeoclimatology Palaeoecology* **306**,
272 58-69 (2011).

- 273 21 Solignac, S., de Vernal, A. & Giraudeau, J. Comparison of coccolith and dinocyst
274 assemblages in the northern North Atlantic: How well do they relate with surface
275 hydrography? *Marine Micropaleontology* **68**, 115-135 (2008).
- 276 22 Rosell-Melé, A., Comes, P., Müller, P. J. & Ziveri, P. Alkenone fluxes and anomalous
277 U-37(K)' values during 1989-1990 in the Northeast Atlantic (48 degrees N 21 degrees
278 W). *Marine Chemistry* **71**, 251-264 (2000).
- 279 23 Kučera M et al. Reconstruction of sea-surface temperatures from assemblages of
280 planktonic foraminifera: multi-technique approach based on geographically constrained
281 calibration data sets and its application to glacial Atlantic and Pacific Oceans.
282 *Quaternary Science Reviews* **24**, 951-998 (2005).
- 283 24 Johannessen, T., Jansen, E., Flatoy, A. & Ravelo, A. C. in *Carbon Cycling in the*
284 *Glacial Ocean: Constrains of the Oceans's Role in Global Change*. (eds R. Zahn, T.F.
285 Pedersen, M.A. Kaminski, & L. Labeyrie) 61-85 (Springer, 1994).
- 286 25 Carstens, J., Hebbeln, D. & Wefer, G. Distribution of planktic foraminifera at the ice
287 margin in the Arctic (Fram Strait). *Marine Micropaleontology* **29**, 257-269 (1997).
- 288 26 Locarnini, R.A. et al. World Ocean Atlas 2013 Volume 1 Temperature. eds Levitus S
289 NOAA Atlas NESDIS 73 40 pp. (2013).
- 290
- 291